

FULLPACK: FULL VECTOR UTILIZATION FOR SUB-BYTE QUANTIZED INFERENCE ON GENERAL PURPOSE CPUs

Hossein Katebi¹ Navidreza Asadi² Maziar Goudarzi¹

ABSTRACT

Although prior art has demonstrated negligible accuracy drop in sub-byte quantization—where weights and/or activations are represented by less than 8 bits—popular SIMD instructions of CPUs do not natively support these datatypes. While recent methods, such as ULPPACK, are already using sub-byte quantization on general-purpose CPUs with vector units, they leave out several empty bits between the sub-byte values in memory and in vector registers to avoid overflow to the neighbours during the operations. This results in memory footprint and bandwidth-usage inefficiencies and suboptimal performance. In this paper, we present memory layouts for storing, and mechanisms for processing sub-byte (4-, 2-, or 1-bit) models that utilize all the bits in the memory as well as in the vector registers for the actual data. We provide compute kernels for the proposed layout for the GEMV (GEneral Matrix-Vector multiplication) operations between weights and activations of different datatypes (e.g., 8-bit activations and 4-bit weights). For evaluation, we extended the TFLite package and added our methods to it, then ran the models on the cycle-accurate gem5 simulator to compare detailed memory and CPU cycles of each method. We compare against nine other methods that are actively used in production including GEMLOWP, Ruy, XNNPack, and ULPPACK. Furthermore, we explore the effect of different input and output sizes of deep learning layers on the performance of our proposed method. Experimental results show $0.96\text{--}2.1\times$ speedup for small sizes and $1.2\text{--}6.7\times$ speedup for mid to large sizes. Applying our proposal to a real-world speech recognition model, Mozilla DeepSpeech, we proved that our method achieves $1.56\text{--}2.11\times$ end-to-end speedup compared to the state-of-the-art, depending on the bit-width employed.

1 INTRODUCTION

Deep Neural Networks (DNN) are showing promising results in various areas such as Natural Language Processing (Devlin et al., 2018), Speech Recognition (Amodi et al., 2016; Hannun et al., 2014), and Computer Vision (He et al., 2016; Ma et al., 2018; Sandler et al., 2018). While DNNs are getting more attention every day, they are compute-intensive. In the past decade, we have witnessed a significant increase in computation power of modern computers, enabling DNN applications. However, running DNN models on mobile devices is still challenging. The community has introduced different quantization schemes to decrease the required computation demands of DNNs. These schemes usually quantize weights and/or activations to 8-bit or 16-bit integers. Recent works

(Gong et al., 2019; Jung et al., 2019; Jacob et al., 2018) demonstrated negligible accuracy loss and considerable performance gains. For instance, (Esser et al., 2020) show that reducing precision of weights and activations to sub-byte has little to no impact on accuracy. In fact, it might even have a positive impact (Banbury et al., 2021) when applying hardware-aware neural architecture search; because in a memory-constrained device, reducing precision of parameters makes room for using more parameters, hence a potential for higher accuracy.

Despite performance gain by sub-byte quantized models in specialized hardware, such models remain infeasible or inefficient on general purpose CPUs due to the lack of support in current popular CPU architectures. Recent works (Won et al., 2022; Reggiani et al., 2022) present novelties to use sub-byte quantized models on CPUs by either adding special hardware to the current processor (Reggiani et al., 2022) or leaving some bits unused when storing and processing the data so as to avoid overflow among adjacent data elements when executing vector instructions (Won et al., 2022). The former needs hardware change and the latter wastes parts of the available memory capacity and bandwidth, and vector processing capability.

¹Department of Computer Engineering, Sharif University of Technology, Tehran, Iran

²Computer Engineering Department, Technical University of Munich, Munich, Germany (navidreza.asadi@tum.de). He was with Sharif University of Technology, Tehran, Iran, while working on this project. Correspondence to: Maziar Goudarzi <goudarzi@sharif.edu>.

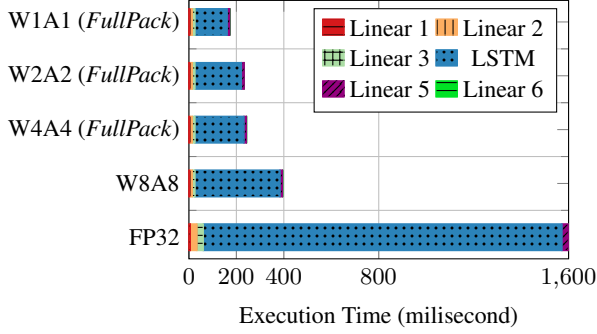


Figure 1. Mozilla DeepSpeech (Mozilla, 2021) per layer execution time breakdown for our W1A1, W2A2, and W4A4 sub-byte quantized, Ruy W8A8 quantized, and Ruy FP32 full precision models.

Existing production-ready frameworks for mobile devices, such as TensorFlowLite and PyTorch are already using low-precision linear algebra libraries to gain performance for quantized models. TensorFlowLite (TFLite) allows to use XNNPack (Google, 2022c), Ruy (Google, 2022b), or GEMMLOWP (Google, 2022a) for quantized models while PyTorch supports QNNPACK (pytorch, 2019) and FBGEMM (Khudia et al., 2021). Nevertheless, these libraries do not support sub-byte quantized models.

We provide mechanisms that enable unmodified off-the-shelf processors, with vector ISA, to use sub-byte quantized models without waste of valuable memory and processing capacity observed in state of the art. We first propose a memory layout to store sub-byte weights and/or activations. Our memory layout is tailored to the vector operations inside the CPU and utilizes the whole space, not leaving even a single bit unused. This enables the vector instructions to extract multiple blocks by consecutive single shifts. We provide various kernels in ARMv8 assembly language to utilize our memory layout and vector operations schedule so as to efficiently implement GEMV on weights and activations using ARM NEON vector instructions. Our performance gains come from better storage and communication (including cache space utilization, memory bandwidth utilization, and memory footprint) as well as improved processing (full utilization of the vector registers and vector processing units) despite some additional instructions needed to extract data from the compressed memory layout. We have implemented our method on TensorFlowLite and have made it available open-source as a fork of TensorFlow¹

In *FullPack*, we decided to focus on GEMV—which is a special case for GEMM—because it did not get enough improvement as the GEMM but is causing significant performance degradation in models utilizing it, such as RNN and LSTM-based models. To support this statement, we eval-

uated Mozilla DeepSpeech (Mozilla, 2021) with different quantization schemes and provided a per-layer execution time breakdown for each model in Figure 1. DeepSpeech includes five multi-batch FullyConnected layers with batch size of 16, and one single-batch LSTM layer. As shown in Figure 1, the LSTM layer is responsible for more than 70% of the whole model execution time. Please note that we can execute sub-byte models on methods that do not explicitly support them, but this leads to no speedup compared to the W8A8 models. So in this paper, we focus on providing speedup while using sub-byte models.

Throughout our experiments, we compare *FullPack* to nine other methods that are available by default or we managed to add to TFLite: (1) *ULPPACK* (Won et al., 2022), which to the best of our knowledge represents the state of the art and is the latest mechanism capable of processing different sub-byte models; four of the other eight methods operate on quantized models (W8A8²): (2) *Ruy for W8A8 models*, (3) *XNNPack for W8A8 models*, (4) *TFLite default for W8A8 models* and (5) *GEMMLOWP*. The rest of the rivals operate on floating point (FP32) models: (6) *Ruy for FP32 models*, (7) *XNNPack for FP32 models*, (8) *TFLite default for FP32 models* and (9) *Eigen* (Eigen).

We selected *Ruy for the W8A8 model* as the baseline in our experiments because this method, along with *XNNPack*, show the best performance among popular publicly available quantization techniques for CPU platforms, but *XNNPack* is not available in several cases and therefore, *Ruy* is the default optimization option on TFLite as well.

We run our experiments on gem5 cycle-accurate processor simulator (Binkert et al., 2011; Lowe-Power et al., 2020). This allowed us to gather detailed reliable execution metrics, such as cache latency, and performance statistics on all the techniques under evaluation. We also evaluate the effect of different cache sizes and hierarchies that might not be available in a real device. All FP32 methods and *ULPPACK* are slower than the main baseline by one or two orders of magnitude. The only two methods that outperformed the baseline, are *XNNPack for W8A8 models* ($2.4\times$ speedup) and *FullPack* ($3.1\times$ speedup). On average, *FullPack* consistently outperforms the other methods when running on models with different sizes.

Our measurements on Raspberry Pi 4 (Section A) also supports our evaluation.

Our contributions are as follows:

- We introduce a packing scheme to efficiently pack multiple sub-byte (<8) elements into a single wider

²Wn: n bits for the weight values, Am: m bits for the activation values; thus, W8A8 case represents 8 bits for each of weights and activations.

¹<https://github.com/shkatebi97/tensorflow>

(≥ 8) value. This packing scheme fully utilizes the memory footprint and bandwidth usage and is designed to reduce extraction overhead.

- Then we propose a set of nine different hand-written GEMV assembly kernels utilizing the introduced packing scheme to effectively process different bit-width (1-, 2-, and 4-bits) and add them to TFLite.
- We evaluate *FullPack* against eight production-ready GEMM/GEMV libraries and the current state-of-the-art, ULPPACK. We also demonstrate the performance improvement of *FullPack* on an end-to-end evaluation of Mozilla DeepSpeech.

The rest of this paper is organized as follows. We discuss the related work on quantized model execution on constrained devices in Section 2. We introduce our method in Section 3 and the results of our evaluations in Section 4. We conclude in Section 5.

2 RELATED WORKS

Literature has extensively demonstrated different techniques of quantizing a deep learning model to sub-byte precision while maintaining or showing negligible drop in accuracy. LSQ (Esser et al., 2020) proposes learning quantization parameters. BitPruning (Nikolić et al., 2020) presents an approach for learning the bit-width of each cluster of values. To make the quantized model even more lightweight, (Alom et al., 2018; Courbariaux et al., 2015) leveraged binary (-1 or 1) values (weight and/or activations) in different types of DNNs. On the other hand, some methods use non-uniform quantization approaches to enhance the performance of their system. MAM (Chang et al., 2021) uses a power-of-2 scheme to quantize the model parameters while GOBO (Zadeh et al., 2020) uses a weight clustering approach, mapping them to only a few unique values. While non-uniform quantization approaches report significant accuracy improvements, these methods do not usually perform well on the commodity CPUs, or are deemed entirely infeasible due to lack of suitable instructions in the CPU ISA.

Utilizing sub-byte quantized models on mobile devices has also gained attention recently. Bison-e (Reggiani et al., 2022) proposed a new hardware extension to RISC-V ISA alongside an approach to pack multiple smaller sub-byte values inside a larger integer. This method utilizes binary segmentation (Pan, 1993) to perform GEMM (General Matrix Multiplication) operations. ULPPACK (Won et al., 2022) utilizes the same method to perform GEMM operations without extending the current ARMv8 ISA. ULPPACK offers two packing schemes to pack the sub-byte values into larger (≥ 16 -bit) integers with an optimized local

accumulation to reduce the impact of data extraction overhead. Both research directions show satisfying speedups even on end-to-end results, nevertheless each has its own drawbacks; Bison-e requires hardware and ISA extensions and thus cannot be used on off-the-shelf general-purpose CPUs, while ULPPACK lacks the ability to fully utilize memory space and bandwidth as well as the full compute capacity of the vector processing units. We provide a replacement that solves both above shortcomings. We use only commodity ARMv8 NEON vector instructions, and our data layout mechanism packs the data elements without spacers in between; despite we need to run more instructions to unpack the data after loaded into vector registers, we show that we still get net positive gain since memory access overhead is the dominant factor in many DNN implementations on today CPUs.

In contrast, we use no additional hardware or new instructions. Our memory layout and assembly kernels are designed for the Vector Unit so that they fully utilize the memory space and execute GEMV operations effectively.

3 METHOD AND IMPLEMENTATION

FullPack consists of two main elements: (1) an efficient packing scheme that fully utilizes the memory bandwidth and space while purpose-built for the processing steps to be applied in the CPU, and (2) handwritten ARMv8-A NEON assembly kernels optimized for each bit-width (1-, 2-, and 4-bits) to take best advantage from the packing scheme. Thus it can also be viewed as a storage-processing co-design scheme.

3.1 Packing Scheme

We design our packing scheme according to the bit-width of weights (activations) and the size of the vector register in the VPU (vector-processing unit). Our method can be used to pack multiple sub-byte (4-, 2-, or 1-bits) parameters in a single byte on any vector register of any size, but we stick to the NEON VPU on ARM CPUs.

The core idea behind our design is minimizing the overhead in the extraction of sub-byte parameters. To achieve this, however, we need to know which sub-byte values we should pack together in a specific byte. The naïve approach packs the adjacent values within an array into a single byte. Algorithm 1 demonstrates the procedure to process data using naïve packing scheme.

In the naïve method, it loads one byte of weight and extracts packed 4-bit values with three shift operations (lines 6-7). Then would load two bytes of corresponding activations (lines 6-7) to multiply them by the corresponding weights and accumulate the result to the corresponding output value (lines 10-11).

Although this method fully utilizes memory bandwidth and space, but it is inefficient to use on VPUs, because the extraction overhead dominates. Noting that NEON ISA performs logical and arithmetic operations at byte level on 16 bytes in parallel using only a single vector instruction, the packing+processing scheme can be co-designed.

For 4-bit quantization, our idea is to pack every two 4-bit elements with stride 16, into a single byte; then, store every 16 of such packs adjacently on consecutive bytes; then again, put every 16 of such 16-byte packs (from the same rows of the matrix) consecutively. This is repeated to fully cover one set of rows of the matrix, and is then repeated again for all other sets of rows of the matrix. Figure 2 demonstrates our proposal for 4-bit values in a 32×16 matrix.

Then at processing time using vector instructions, the above arrangement allows to load 16-bytes of data at once into the vector registers, and extract every 16 originally-subsequent elements by simple vector-shift operations. Note that the 16-bytes data is read only once from memory, but it contains 32 elements of the original 4-bit values; compare that with ULPPack storage where spacer bits are put between elements, and hence, same 16-byte read from memory yields smaller amount of useful data.

Thus, VPU can extract values from 1 to 16 with two shifts (one logical shift to the left and one arithmetic shift to the right to do the sign-extension), and then the 16th to 32nd values with one arithmetic shift to the right to do the sign-extension. The reason behind the two required shifts for extraction of values 1-16 is that by applying two shifts, we

Algorithm 1 Naïve method for the W4A8 model using FMA

Input: weights and k -dimensional activation as W and A with 8 and 8 bit width

Output: z -dimensional output O

```

1:  $i \leftarrow 0$ 
2: for  $i < z$  do
3:    $j \leftarrow 0$ 
4:    $O[i] \leftarrow 0$ 
5:   for  $j < k$  do
6:      $W_0 \leftarrow (W[i] \gg 4) \ll 4$ 
7:      $W_1 \leftarrow W[i] \ll 4$ 
8:      $A_0 \leftarrow A[i]$ 
9:      $A_1 \leftarrow A[i + 1]$ 
10:     $O[i] \leftarrow \text{FMA}(W_0, A_0, O[i])$ 
11:     $O[i] \leftarrow \text{FMA}(W_1, A_1, O[i])$ 
12:     $j \leftarrow j + 2$ 
13:  end for
14:   $O[i] \leftarrow \text{ElementWiseAdd}(V_2)$ 
15:   $i \leftarrow i + 1$ 
16: end for
17: return  $O$ 
    
```

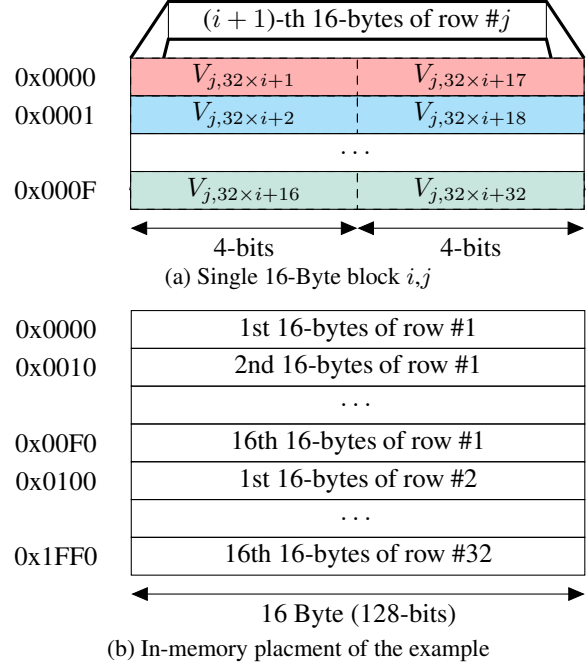


Figure 2. Proposed packing scheme for an example matrix of size 32×16 with 4-bit values.

can mask and sign-extend the values but with only masking, we can not sign-extend values. On the other hand, these two shifts can be performed in place. Therefore, there is no need for another VPU register.

Our packing scheme can pack 1-bit and 2-bit parameters as well. For 1-bit values, we pack eight 1-bit values with stride 16 in a single byte, and thus 128 original 1-bit values are loaded from memory into a vector register by a single 16-byte vector load instruction. Similarly, for 2-bit values, there would be four values in a single byte and 64 values loaded from memory into a vector register. We can selectively apply our packing scheme to weights or activations or both. Also, one can utilize any VPU with any bit width by extending the above scheme. Obviously, with larger vector registers, we can fit more values inside a single vector. However, for scalable vector schemes such as ARM SVE and RISC-V RVV, our processing scheme needs adjustments since the processor vector length is not known statically; this remains as part of our future work.

3.2 GEMV Kernels

To perform matrix multiplication on weights and activations, we provide a series of kernel functions. Each function is specialized to process a specific model type. The supported types are W8A4, W4A8, W4A4, W2A8, W8A2, W2A2, W1A8, W8A1, and W1A1.

Algorithm 2 shows how we process the W4A8 model using Fused Multiply and Add (FMA) instruction. In each function, we load a vector-size block of data (weights or

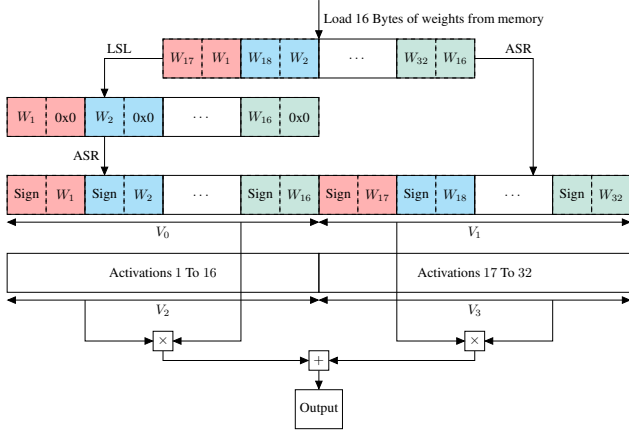


Figure 3. Processing a block of weights (16 Bytes) with the proposed method for the W4A8 model. V_0 , V_1 , V_2 , and V_3 are four sample vector registers and the output is a scalar accumulated in the V_4 register.

activations) into a vector register and if needed, based on the quantization bit-width of the model, we extract/load the values into one or more vector registers (lines 6-11), and then we multiply the extracted weights and activations and accumulate the resulting products in a vector register (lines 12-13). Figure 3 tries to illustrate the processing of a block of weights and the corresponding activations for the model. As depicted, the weights are loaded from memory into a vector register, and then demultiplexed into two vector registers (V_0 and V_1). For extracting the weights W_1 to W_{16} of this block, we need two shift operations: one Logical Shift Left (LSL) for masking and one Arithmetic Shift Right (ASR) for sign extension. For extracting the other 16 weights (W_{17} to W_{32}) from the original vector register, only one Arithmetic Shift Right (ASR) operation is needed for sign extension. After preparing the weights, we load 32 corresponding activations into two vectors, V_2 and V_3 , and then process the dot-product of 32 weights and activations in those vector registers.

4 EVALUATION

We implemented and integrated our method into TFLite and compared it to eight production-ready libraries, mostly written in assembly by industry experts, and available in TFLite, as well as *ULPPACK*.

Table 1. *gem5* simulation setup

CPU Type	modified ex5_big
Architecture	ARMv8-A
Micro-Architecture	Single core @ 2.45GHz (max freq.)
L1 Cache (per core)	128KB I\$ + 128KB D\$
L2 Cache [×] (Shared)	2 MB
L3 Cache (Shared)	8 MB (where employed)
RAM	4GB (LPDDR3x @ 1600MHz)

[×]: Size may alter or get removed based on the experiment.

Algorithm 2 Proposed method for the W4A8 model using FMA and Vector ISA

Input: Packed weights and k -dimensional activation as W and A with 4 and 8 bit width

Output: z -dimensional output O

```

1:  $i \leftarrow 0$ 
2: for  $i < z$  do
3:    $j \leftarrow 0$ 
4:    $V_4 \leftarrow 0$ 
5:   for  $j < k$  do
6:      $V_0 \leftarrow$  load 16 bytes of  $W$  and increment
7:      $V_1 \leftarrow$  ArithmeticShiftRight( $V_0$ , 4)
8:      $V_0 \leftarrow$  LogicalShiftLeft( $V_0$ , 4)
9:      $V_0 \leftarrow$  ArithmeticShiftRight( $V_0$ , 4)
10:     $V_2 \leftarrow$  load 16 bytes of  $A$  and increment
11:     $V_3 \leftarrow$  load 16 bytes of  $A$  and increment
12:     $V_4 \leftarrow$  FMA( $V_0$ ,  $V_2$ ,  $V_4$ )
13:     $V_4 \leftarrow$  FMA( $V_1$ ,  $V_3$ ,  $V_4$ )
14:     $j \leftarrow j + 32$ 
15:  end for
16:   $O[i] \leftarrow$  ElementWiseAdd( $V_4$ )
17:   $i \leftarrow i + 1$ 
18: end for
19: return  $O$ 
    
```

4.1 Experiments Setup

We evaluated all nine methods on the cycle-accurate *gem5* simulator (Binkert et al., 2011; Lowe-Power et al., 2020) (Table 1). Except in §4.4 where we evaluate different L2 cache sizes and also add an L3 cache, the default configurations for the rest of the experiments include a 2MB L2 cache as the last level cache.

Additionally, we evaluated *FullPack* on Raspberry Pi 4 (§ A), and compared it with the other methods on Fully-Connected layers of eleven well-known convolutional neural networks.

We employed TFLite benchmarking tool (TensorFlow, 2021) which we built using `-c opt` Bazel flag that enables `-O3` flag on compile-time. This tool allows us to easily select the method we want to run with run-time flags. However, *GEMMLOWP* and *Eigen* needed a compile-time flag to be activated to replace the default execution path.

We evaluated our proposal against the following methods.

Ruy for W8A8 models. (Ruy-W8A8): *Ruy* is the default method in TFLite when the caching is enabled. This method is developed by Google and is the fastest among all rivals, except *XNNPACK*.

XNNPack. (XNNPack-W8A8): This method by Google and Facebook is often the fastest method in TFLite, but it requires heavy preprocessing and does not support all operations of TFLite; this causes slowdown when moving data between supported and not supported operators. In addi-

tion, our focus is on the efficacy of the packing scheme. Thus, the other ISA-specific instructions, e.g., prefetching are out of the scope of this work. `XNNPack-W8A8` is written in assembly.

TFLite default for W8A8 models. (`TFLite-W8A8`): This method is the default method when the caching is disabled and is written in C/C++ with compiler intrinsics.

GEMMLOWP. (`GEMMLOWP-W8A8`): Another library in TFLite for GEMM and GEMV operations that is not available by default but can be embedded into the binaries using a compile-time flag. Unlike `Ruy` and `XNNPACK`, this library only supports `W8A8` models and does not support 32-bit floating point (`FP32`) models. `GEMMLOWP` is also handwritten in assembly.

Ruy for FP32 models. (`Ruy-FP32`): This method is also from the `Ruy` library but for processing `FP32` models.

XNNPack for FP32 models. (`XNNPack-FP32`): This method is also from the `XNNPACK` library but for processing `FP32` models.

TFLite default for FP32 models. (`TFLite-FP32`): This method is the default execution mechanism that TFLite employs for processing `FP32` models while caching is not enabled.

Eigen. (`Eigen-FP32`): This method only supports `FP32` models and like `GEMMLOWP`, is not available by default, but can be added to the binary using a compile-time flag.

ULPPACK.³ (`ULPPACK-W3A3`, `ULPPACK-W2A2`, `ULPPACK-W1A1`): `ULPPACK` supports sub-byte models with different bit-widths for activations and weights independently. However, we only selected models with the same bit-width for activations and weights for brevity. Also note that according to the authors (Won et al., 2022), `ULPPACK` does not gain speedup with `W4A4`, `W5A5`, `W6A6`, and `W7A7` models. Further note that `ULPPACK` only implements GEMM and does not have any GEMV-specific kernel, so in each inference experiment, we pass `ULPPACK` an input with 8 batches with the same values; we call this reduced version, `ULPPACK-`.

The Baseline. Although `XNNPack-W8A8` was often the fastest among the rivals, but since it is not available for some cases of our studies or degrades performance for the same, we chose `Ruy-W8A8` as the baseline, and normalize all results against it.

4.2 Performance Comparison

We first study the speedup on different input and output sizes of a `FullyConnected` layer. Figure 4 depicts the results. Except `FullPack` for `W4A8` and `XNNPack-W8A8`, all other methods are slower than the baseline (`Ruy-W8A8`). `XNNPack-W8A8`, in contrast to our method, gains more speedup for smaller models while our method outperforms it for larger models. This is mainly because `FullPack` uses less memory bandwidth which is more visible on larger inputs. We will discuss this more in §4.3.1. As we can see in Figure 4, on average, our method for `W4A8` can reach a performance gain of $2.44\times$.

4.3 What to Quantize? Weights, Activations, or Both?

Another aspect is the effect of different quantization schemes. In §4.2, we evaluated our method on the `W4A8` model which only utilizes quantization on the weights of the model, however we can also quantize only the activations (`W8A4`), or weights and activations together (`W4A4`).

Different assembly kernels to process the GEMV for each model are required. To run `W8A4` models, we apply our packing scheme only on activations while for `W4A4` models, we apply our packing scheme on both activations and weights.

Figure 5 illustrates the result of running our method on `W8A4` and `W4A4` models. Applying sub-byte quantization on the weights will cause a speedup of $2.44\times$ while applying the same quantization only on activations improves the performance by $1.92\times$. However, if we apply sub-byte quantization on both weights and activations, the performance will improve by $2.48\times$ which is only about $1.02\times$ faster than the model that only has sub-byte weights.

The reason behind this is that total size of weight elements in GEMV operations is in general bigger than the activations. Consequently, when we quantize the weights, memory bandwidth usage drops significantly compared to quantizing the activations.

By taking a closer look at Figures 4a, 5a, and 5b, a diagonal boundary from the top right to the bottom left of each table is noticeable and demonstrates higher speedups compared to other cases. From this boundary to the left (before the boundary), we mostly observe a reduction in speedup. To the right of the boundary, however, we observe higher speedup compared to the left-hand side, but

³`ULPPACK` does not have an open-source code base. We contacted the authors and they kindly sent us the codes; we cordially acknowledge and appreciate that. We then ported it to TFLite ourselves for comparisons, so beware of any potential deficiencies inadvertently introduced.

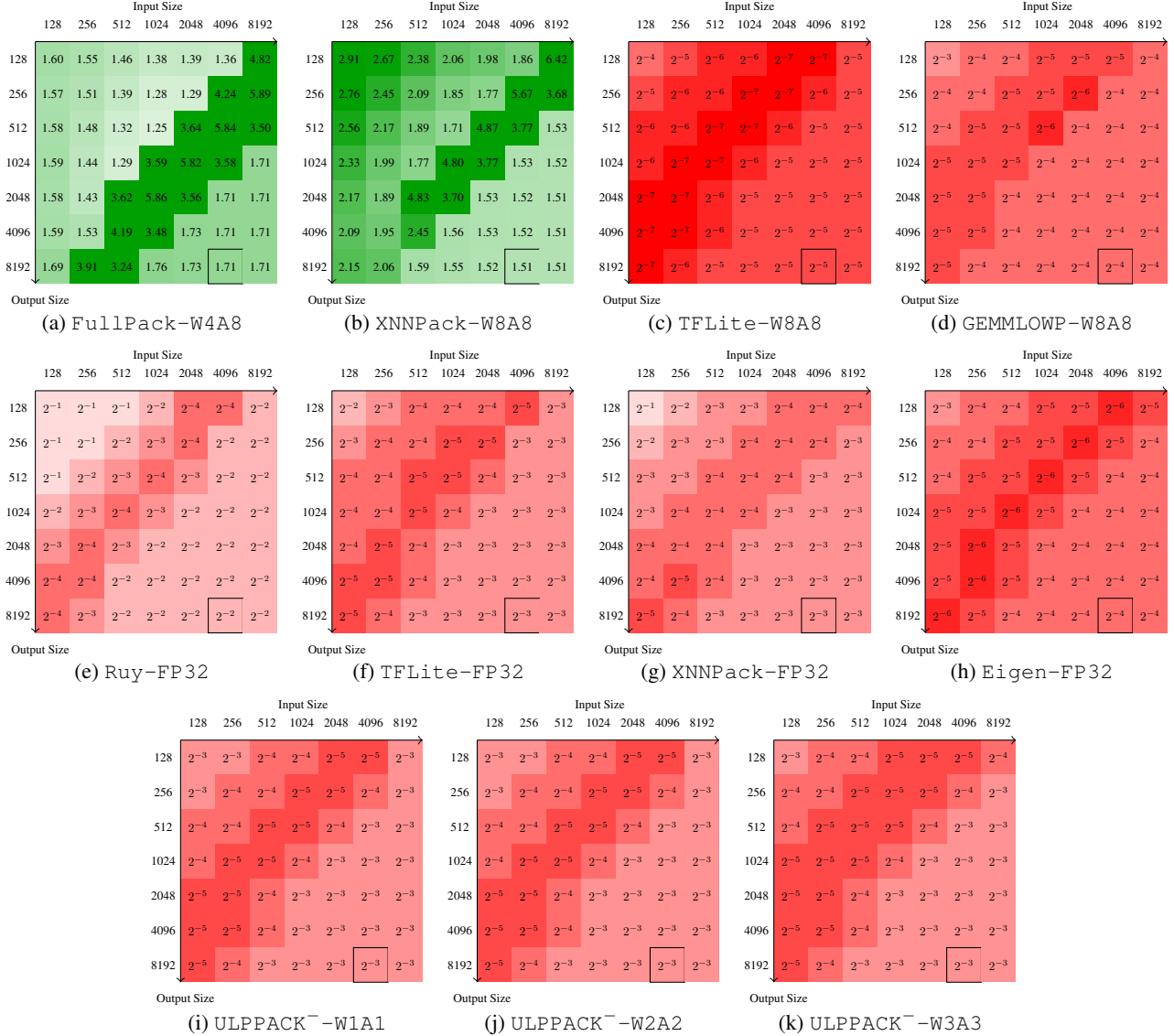


Figure 4. Performance comparison (Speedup; $T_{baseline} / T_{case}$) of different methods on various IO sizes of a FullyConnected layer against the baseline (Ruy-W8A8). The number in the cell reports the speedup. Red, white, and green blocks indicate slow down, no improvement, and speed up, respectively. The cells with black borders correspond to the IO size of the LSTM layer in Mozilla DeepSpeech.

it saturates: almost no change with respect to the modification of input/output sizes. This can be justified by the effect of caches which we discuss in §4.3.1.

4.3.1 Last-Level Cache Behavior

To investigate the mentioned observation, we evaluate the Last Level Cache (LLC) behavior throughout the execution of each model. Figure 6 demonstrates the LLC behavior on models of different sizes. Using sub-byte weights (Figure 6a), the LLC accesses are reduced by 50% for larger models, while sub-byte activations barely reduce LLC accesses for these models (Figure 6e for W8A4 and Figure 6i for W4A4).

However, if we take a closer look at the nodes to the right of the diagonal of W4A8 models in Figure 6, it illustrates that accesses of our method (6a) are 50% fewer than the baseline, and misses (6b) are about 90% fewer than the baseline. This causes the miss rate (6c) to be 70-80% lower than the baseline. Looking at these sizes and the L2 cache size in Table 1, we find out that in these sizes, our weight matrix fits in the L2 cache but the W8A8 weight matrix does not. This causes the baseline to suffer from ~99% L2 cache miss rate. Figure (6d) depicts LLC cache miss latency. It shows that our method reduces the cache miss latency by 80-90% on these models.

Furthermore, after the diagonal boundary, the LLC ac-

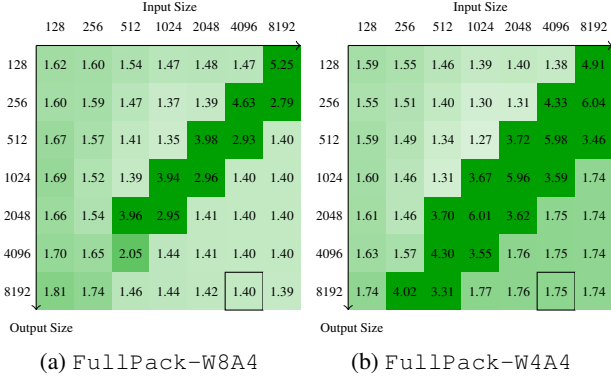


Figure 5. The effect of quantizing weights and/or activations on the performance (Speedup) of our method on different sizes.

cesses (6a) and misses (6b) are both reduced by 50%, and thus the same miss rate (6c) as the baseline. This demonstrates the case where our method takes best advantage from its lower memory bandwidth usage and reduces the LLC miss latency (6d) by $\sim 50\%$.

Note how W8A4 model has almost same number of accesses, misses (and thus miss rate) and LLC miss latency as the baseline at IO sizes to the right of the diagonal boundary (6e, 6f, 6g, and 6h). This confirms that activation-quantization is not as effective as weight-quantization here.

4.4 Different Sizes of Last-Level Cache

In the previous Section, we showed that the formation of a maximum-speedup boundary obtained by our method is an effect of the Last-Level Cache capacity; when even the packed data does not fit the LLC, we start to lose some speedup while still performing better than Ruy-W8A8. We further evaluated the above behavior on our W4A4 model vs. baseline under various cache sizes and cache hierarchies. Figure 7 presents the results; at higher LLC sizes or when an L3 cache is introduced, the maximum-speedup boundary moves to the higher IO sizes. This further confirms and also quantifies the LLC effect on our obtained speedups. Even with L2 and L3 caches removed (7d), the same above effect is observed but at smaller sizes since now L1 size is the limit. Note that the inference latency differs when cache size and structure changes; the above figures only depict the *speedup* vs. baseline in each case.

4.5 What If We Use Fewer Bits?

In the previous experiments, we only evaluated our method on 4-bit quantized models. Here, we evaluate the narrower bit widths for weights and/or activations. Figure 8 shows speedups and instructions count of our method on W2A2 and W1A1 models w.r.t. our method on W4A4. Using fewer bits expands the maximum-speedup boundary region and also improves the obtainable speedup beyond that

boundary. However, if we observe figures 8c and 8d we can see that compared to W4A4, FullPack for W2A2 models uses negligible fewer instructions but W1A1 models requires more instructions: $1.03\times$ for W2A2, and $0.8\times$ for W1A1 models compared to W4A4 models. Such behavior leads to a higher speedup on larger models compared to W4A4: $1.23\times$ for W2A2, and $1.17\times$ for W1A1 models.

4.6 End-To-End Performance

For the end-to-end performance, we evaluate all the methods on Mozilla DeepSpeech (Mozilla, 2021). This model contains five multi-batch Fully Connected layers with 16 batches and one multi-batch LSTM layer with 16 batches which is unrolled to 16 consecutive single-batch LSTM layers. The model architecture is shown in Figure 9. Only LSTM layers are single-batch. These single-batch layers are the layers that utilize GEMV operations; other layers use GEMM operations. However, as depicted in Figure 1, the LSTM layer consumes more than 70% of the whole inference time. Since our algorithm is for the GEMV operations, we apply it only on the LSTM layer and we use Ruy-W8A8 (the baseline) for the GEMM operations (multi-batch layers).

Figure 10 illustrates end-to-end breakdown of per-layer execution time of the DeepSpeech model for each method, extracted with the TFLite benchmarking tool per operation profiling. Regarding the total execution time, we observe that FullPack for all three models outperforms all the others despite the fact that all of our improvement comes only from the LSTM layer. Our method can achieve an end-to-end speedup of $1.56\text{-}2.11\times$ and $1.23\text{-}1.66\times$ compared to the best rivals, namely (Ruy-W8A8) and XNNPack-W8A8 respectively.

For more results of the evaluation of all methods on real-world models on a real device, please refer to the section A of the appendix.

4.7 On-Device Performance

For evaluation on the real devices, we selected Fully Connected layers of eleven well-known Convolutional Neural Networks (CNNs), namely DenseNet201, EfficientNetV2L, InceptionV3, InceptionResNetV2, MobileNetV2, NASNetLarge, RegNetY320, ResNet152, ResNet152V2, VGG19, and Xception. These layers in CNNs utilize GEMV, which is the main focus of this paper, while the other layers, including convolutional layers, are implemented with GEMM operations. We executed each of them using TFLite benchmarking tool, for 10 warmup iterations and 100 main iterations on Raspberry Pi 4 (Table 2) and averaged over the main iterations for the results. Figure 11 (in Appendix) demonstrates the speedup of each method over the baseline, Ruy-W8A8. The results further support our

FullPack: Full Vector Utilization for Sub-Byte Quantized Inference on General Purpose CPUs

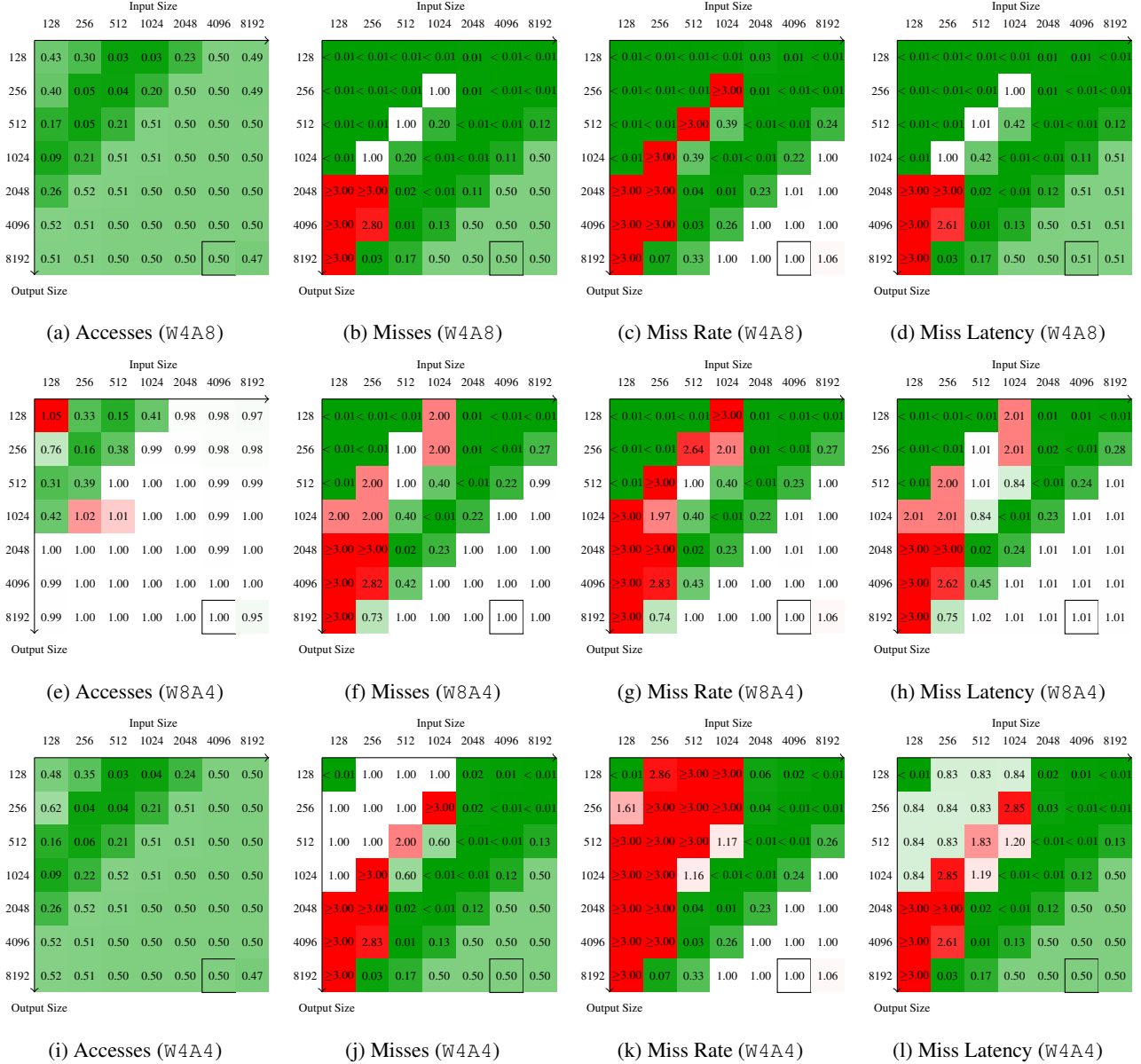


Figure 6. Last Level (L2) Cache metrics ($M_{case}/M_{baseline}$), including access, miss, miss rate, and access latency of our method for W4A8, W8A4, and W4A4 models compared to the main baseline. Values from 0.0 to 1.0 indicate a reduction with 0.0 being almost reduced to 0 ($\infty\times$ reduction) or more than $100\times$ reduction and 1.0 being no reduction or being the same. However, values more than 1.0 demonstrate an increase. The greater the value, the more increase in the metric.

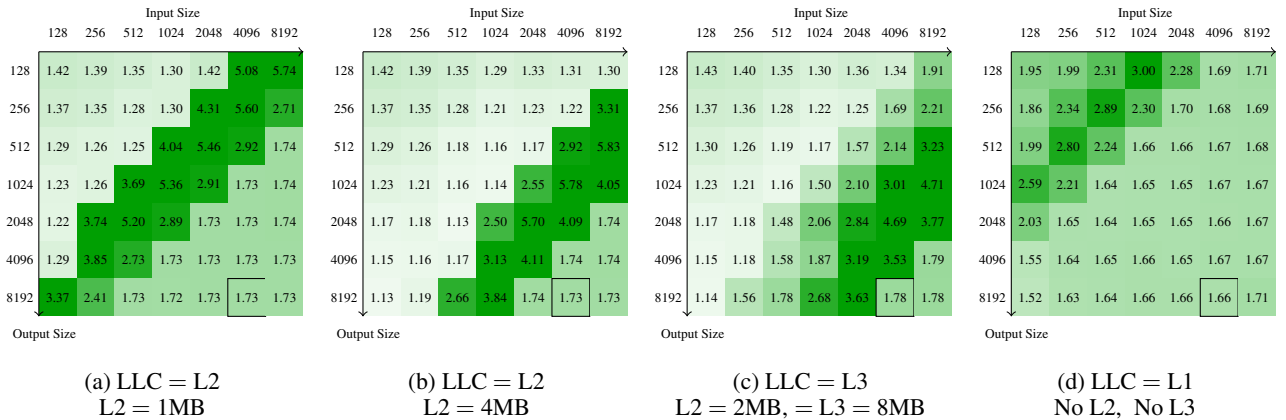


Figure 7. Effect of different sizes and hierarchies of Last Level Cache (LLC) on the performance (speedup) of FullPack for W4A4 models compared to the baseline.

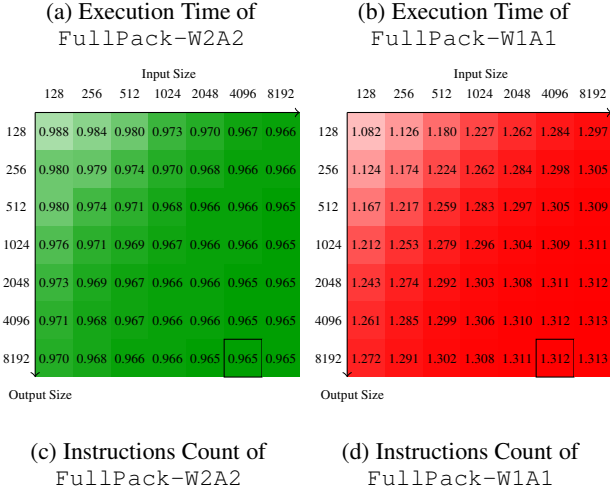
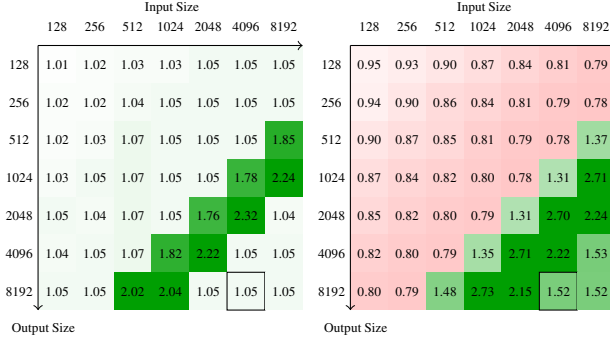


Figure 8. The effect of different quantization bit-widths on the speedups against $W4A4$ (T_{W4A4} / T_{case}) and the increase in executed Instructions Count w.r.t. $W4A4$ (I_{case} / I_{W4A4}) obtained by our method.

evaluation on *gem5* as we achieve on average $1.2\times$, $1.5\times$ and $1.43\times$, and up to $1.38\times$, $1.69\times$ and $1.62\times$ speedup over the main baseline for W1A1, W2A2 and W4A4, respectively, while outperforming the other rivals.

5 CONCLUSION

To tackle the bandwidth and capacity wastage of the latest solutions for sub-byte DNN models on constrained devices, we introduced a storage-processing co-design packing scheme for fixed-width vector instructions of commodity processors such as ARM’s NEON architecture; our solution needs no hardware extension, and fully utilizes the

Table 2. Raspberry Pi 4 Model B Specifications

CPU Type	Broadcom BCM2711
Architecture	ARMv8-A
Micro-Architecture	4× (Cortex-A72) core @ 2.45GHz (max freq.)
L1 Cache (per core)	32KB I + 32KB D
L2 Cache (Shared)	1 MB
RAM	4GB (LPDDR4 @ 2400MHz)

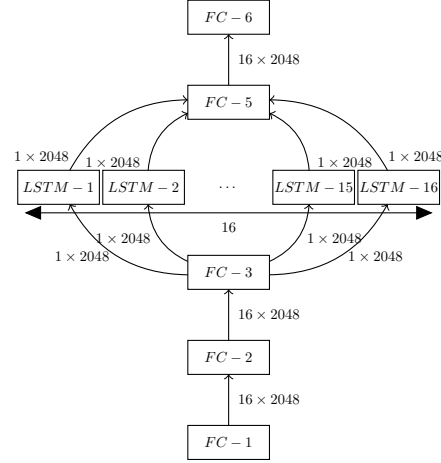


Figure 9. The network architecture of Mozilla DeepSpeech.

consumed memory bandwidth and memory footprint to respectively transfer and store only useful data. These packing schemes alongside their corresponding assembly kernels reduce expensive cache-misses, and thus improve performance despite needing some additional vector instructions for unpacking the data in the vector registers. We implemented our scheme for the GEMV operation, common in fully-connected and other layers, of DNN models and provide it open source to the community. We evaluated *FullPack* against nine other well-known techniques including the current state-of-the-art in the literature (ULP-PACK) as well as industry (*Ruy*, *XNNPACK*, and *GEMM-LOWP*), and showed on cycle-accurate processor simulator that on average, *FullPack* consistently outperforms all rivals. *FullPack* achieves $2.35\times$ speedup against the baseline, *Ruy*-W8A8. For end-to-end evaluation, we applied all methods on Mozilla DeepSpeech and showed that *FullPack* outperforms all the others and provides $1.2 - 1.4\times$ speedup over the closest rival, *XNNPACK*.

REFERENCES

- Alom, M. Z., Moody, A. T., Maruyama, N., Van Essen, B. C., and Taha, T. M. Effective quantization approaches for recurrent neural networks. In *2018 international joint conference on neural networks (IJCNN)*, pp. 1–8. IEEE, 2018.
- Amodei, D., Ananthanarayanan, S., Anubhai, R., Bai, J., Battenberg, E., Case, C., Casper, J., Catanzaro, B., Cheng, Q., Chen, G., et al. Deep speech 2: End-to-end speech recognition in english and mandarin. In *International conference on machine learning*, pp. 173–182. PMLR, 2016.
- Banbury, C., Zhou, C., Fedorov, I., Matas, R., Thakker, U., Gope, D., Janapa Reddi, V., Mattina, M., and Whatmough, P. Micronets: Neural network architectures for

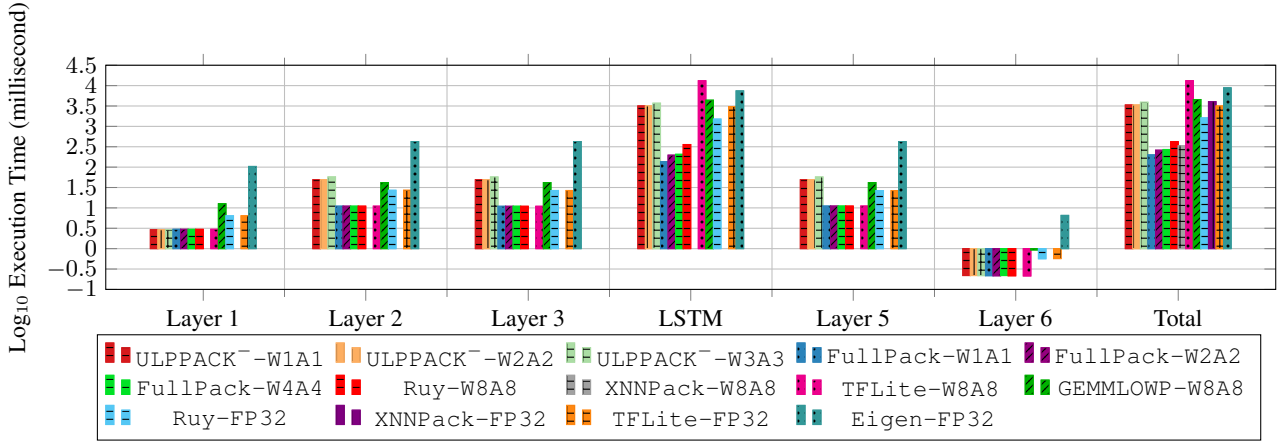


Figure 10. End-To-End evaluation on Mozilla DeepSpeech (Mozilla, 2021) by per layer execution time breakdown, for all of the methods except XNNPACK, because it does not allow per layer breakdown. FullPack does not support GEMM, so we used Ruy-W8A8 for processing the GEMM operations.

deploying tinyml applications on commodity microcontrollers. *Proceedings of Machine Learning and Systems*, 3:517–532, 2021.

Binkert, N., Beckmann, B., Black, G., Reinhardt, S. K., Saidi, A., Basu, A., Hestness, J., Hower, D. R., Krishna, T., Sardashti, S., et al. The gem5 simulator. *ACM SIGARCH computer architecture news*, 39(2):1–7, 2011.

Chang, S.-E., Li, Y., Sun, M., Shi, R., So, H. K.-H., Qian, X., Wang, Y., and Lin, X. Mix and match: A novel fpga-centric deep neural network quantization framework. In *2021 IEEE International Symposium on High-Performance Computer Architecture (HPCA)*, pp. 208–220. IEEE, 2021.

Courbariaux, M., Bengio, Y., and David, J.-P. Binaryconnect: Training deep neural networks with binary weights during propagations. *Advances in neural information processing systems*, 28, 2015.

Devlin, J., Chang, M.-W., Lee, K., and Toutanova, K. Bert: Pre-training of deep bidirectional transformers for language understanding. *arXiv preprint arXiv:1810.04805*, 2018.

Eigen. Eigen. <http://eigen.tuxfamily.org>. [Online; accessed 23-October-2022].

Esser, S. K., McKinstry, J. L., Bablani, D., Appuswamy, R., and Modha, D. S. Learned step size quantization. 2020.

Gong, R., Liu, X., Jiang, S., Li, T., Hu, P., Lin, J., Yu, F., and Yan, J. Differentiable soft quantization: Bridging full-precision and low-bit neural networks. In *Proceedings of the IEEE/CVF International Conference on Computer Vision*, pp. 4852–4861, 2019.

Google. google/gemmlowp: Low-precision matrix multiplication. <https://github.com/google/gemmlowp>, September 2022a. [Online; accessed 21-September-2022].

Google. google/ruy. <https://github.com/google/ruy>, September 2022b. [Online; accessed 21-September-2022].

Google. google/XNNPACK: High-efficiency floating-point neural network inference operators for mobile, server, and Web. <https://github.com/google/XNNPACK>, September 2022c. [Online; accessed 21-September-2022].

Hannun, A., Case, C., Casper, J., Catanzaro, B., Diamos, G., Elsen, E., Prenger, R., Satheesh, S., Sengupta, S., Coates, A., et al. Deep speech: Scaling up end-to-end speech recognition. *arXiv preprint arXiv:1412.5567*, 2014.

He, K., Zhang, X., Ren, S., and Sun, J. Deep residual learning for image recognition. In *Proceedings of the IEEE conference on computer vision and pattern recognition*, pp. 770–778, 2016.

Jacob, B., Kligys, S., Chen, B., Zhu, M., Tang, M., Howard, A., Adam, H., and Kalenichenko, D. Quantization and training of neural networks for efficient integer-arithmetic-only inference. In *Proceedings of the IEEE conference on computer vision and pattern recognition*, pp. 2704–2713, 2018.

Jung, S., Son, C., Lee, S., Son, J., Han, J.-J., Kwak, Y., Hwang, S. J., and Choi, C. Learning to quantize deep networks by optimizing quantization intervals with task loss.

- In *Proceedings of the IEEE/CVF Conference on Computer Vision and Pattern Recognition*, pp. 4350–4359, 2019.
- Khudia, D., Huang, J., Basu, P., Deng, S., Liu, H., Park, J., and Smelyanskiy, M. Fbgemm: Enabling high-performance low-precision deep learning inference. *arXiv preprint arXiv:2101.05615*, 2021.
- Lowe-Power, J., Ahmad, A. M., Akram, A., Alian, M., Am-slinger, R., Andreozzi, M., Armejach, A., Asmussen, N., Beckmann, B., Bharadwaj, S., et al. The gem5 simulator: Version 20.0+. *arXiv preprint arXiv:2007.03152*, 2020.
- Ma, N., Zhang, X., Zheng, H.-T., and Sun, J. Shufflenet v2: Practical guidelines for efficient cnn architecture design. In *Proceedings of the European conference on computer vision (ECCV)*, pp. 116–131, 2018.
- Mozilla. mozilla/DeepSpeech: DeepSpeech is an open source embedded (offline, on-device) speech-to-text engine which can run in real time on devices ranging from a Raspberry Pi 4 to high power GPU servers. <https://github.com/mozilla/DeepSpeech>, November 2021. [Online; accessed 22-September-2022].
- Nikolić, M., Hacene, G. B., Bannon, C., Lascorz, A. D., Courbariaux, M., Bengio, Y., Gripon, V., and Moshovos, A. Bitpruning: Learning bitlengths for aggressive and accurate quantization. *arXiv preprint arXiv:2002.03090*, 2020.
- Pan, V. Binary segmentation for matrix and vector operations. *Computers & Mathematics with Applications*, 25 (3):69–71, 1993.
- pytorch. pytorch/QNNPACK: Quantized Neural Network PACKage - mobile-optimized implementation of quantized neural network operators. <https://github.com/pytorch/QNNPACK>, August 2019. [Online; accessed 21-September-2022].
- Reggiani, E., Lazo, C. R., Bagué, R. F., Cristal, A., Olivieri, M., and Unsal, O. S. Bison-e: a lightweight and high-performance accelerator for narrow integer linear algebra computing on the edge. In *Proceedings of the 27th ACM International Conference on Architectural Support for Programming Languages and Operating Systems*, pp. 56–69, 2022.
- Sandler, M., Howard, A., Zhu, M., Zhmoginov, A., and Chen, L.-C. Mobilenetv2: Inverted residuals and linear bottlenecks. In *Proceedings of the IEEE conference on computer vision and pattern recognition*, pp. 4510–4520, 2018.
- TensorFlow. tensorflow/README.md at r2.8 · tensorflow/tensorflow. <https://github.com/tensorflow/tensorflow/blob/r2.8/tensorflow/README.md>, November 2021. [Online; accessed 28-September-2022].
- Won, J., Si, J., Son, S., Ham, T. J., and Lee, J. W. Ulppack: Fast sub-8-bit matrix multiply on commodity simd hardware. *Proceedings of Machine Learning and Systems*, 4: 52–63, 2022.
- Zadeh, A. H., Edo, I., Awad, O. M., and Moshovos, A. Gobo: Quantizing attention-based nlp models for low latency and energy efficient inference. In *2020 53rd Annual IEEE/ACM International Symposium on Microarchitecture (MICRO)*, pp. 811–824. IEEE, 2020.

A ON-DEVICE MEASUREMENTS

A complete demonstration of the results of our evaluation on fully connected layers of eleven different well-known CNN models are available in Figure 11.

B DETAILED EXECUTION METRIC ANALYSIS

Here, we provide more detailed information about the execution of each method. As depicted in Figure 4, *FullPack* outperforms the baseline, *Ruy-W8A8*. One may expect that with narrower bit-width, the speedup of *FullPack* to get better, but as discussed in § 4.3 and § 4.5, this is true only for *FullPack-W2A2* and not for *FullPack-W1A1*. As previously mentioned, the reason is that the instructions overhead becomes bottleneck in execution of *FullPack-W1A1*. For deeper inspection, we reported Instructions Count of each method for each model against the main baseline, *Ruy-W8A8* (Figure 12).

As we see, only when we quantize the activations, we still have $0.73\times$ instructions compared to the baseline. The reason is that *Ruy-W8A8* needs more preprocessing to prepare the data for processing with respect to *FullPack*. However, *XNNPack-W8A8* needs way less instructions compared to both *FullPack* and *Ruy-W8A8*, $0.68\times$ of *Ruy-W8A8*.

This, however, does not explain the reason behind why *FullPack* is faster than *XNNPack-W8A8* for models with larger sizes. To investigate more, we evaluated Instructions Per Cycle (IPC) for each method. Figure 13 reports our results. Here, *FullPack* has better IPC than the baseline for almost all models and all sizes. However, if we compare the IPC of *XNNPack-W8A8* with *FullPack* we can observe that *FullPack* has better IPC than the *XNNPack-W8A8* for larger sizes of all the models, except *W8A4*, which causes *FullPack* to be faster than *XNNPack-W8A8*, even with more executed instructions.

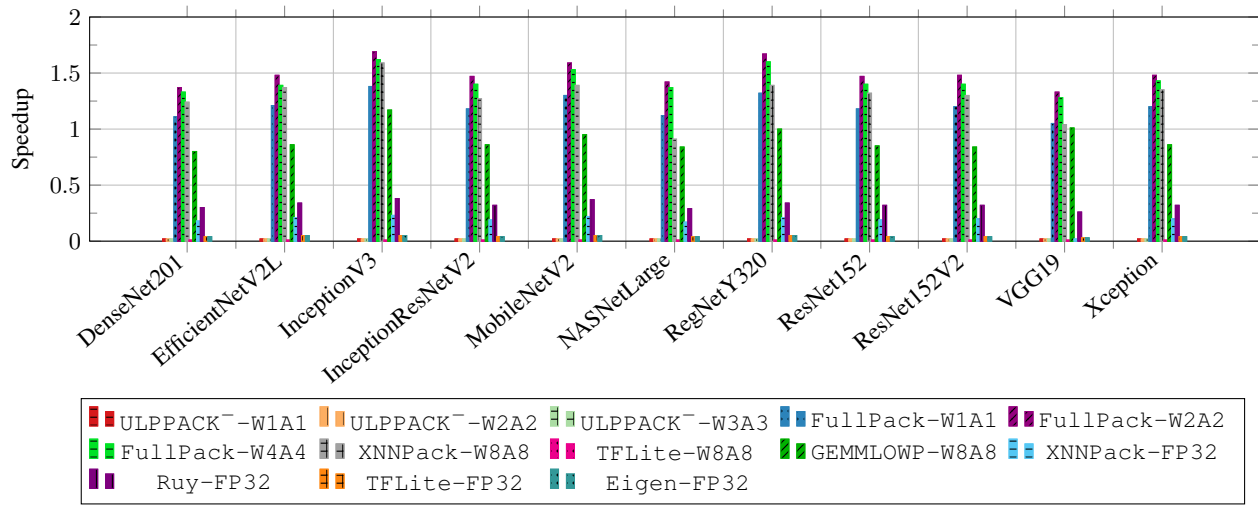


Figure 11. Speedup of each method against Ruy-W8A8 on Fully Connected layers of a few well-known Convolutional Neural Networks on Raspberry Pi 4 Model B.

FullPack: Full Vector Utilization for Sub-Byte Quantized Inference on General Purpose CPUs



Figure 12. Instruction Count comparison (Increase; $I_{case}/I_{baseline}$) of different methods on various IO sizes of a FullyConnected layer against the baseline (Ruy-W8A8). The number of cells reports the increase multiplier.

FullPack: Full Vector Utilization for Sub-Byte Quantized Inference on General Purpose CPUs

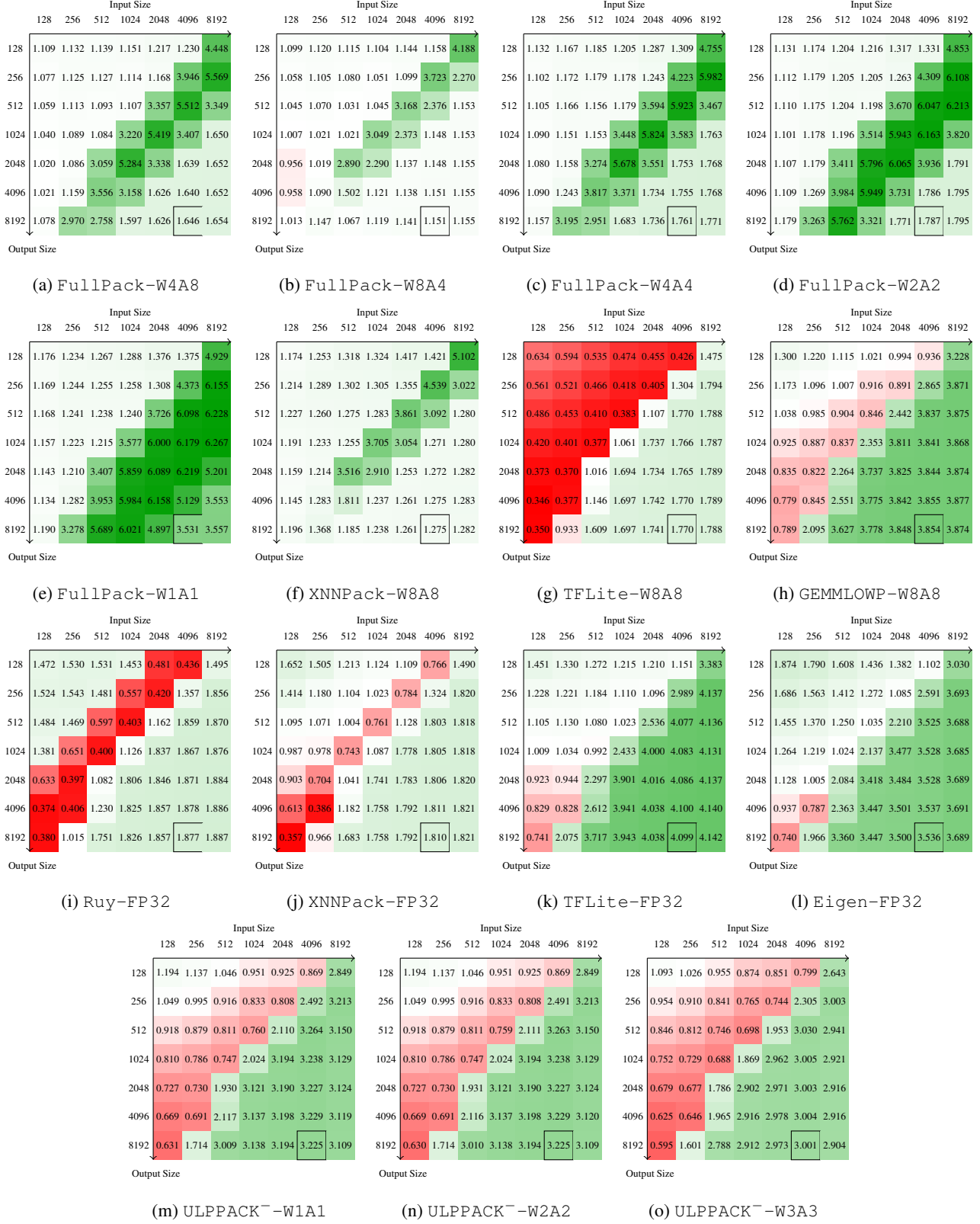


Figure 13. IPC (Instruction Per Cycle) comparison (Increase; $IPC_{case}/IPC_{baseline}$) of different methods on various IO sizes of a FullyConnected layer against the baseline (Ruy-W8A8). The number of cells reports the increase multiplier.